Learning about threat from friends and strangers is equally effective: an fMRI study on observational fear conditioning

Anna M. Kaźmierowska[1, 2, †], Michał Szczepanik[1, 2, †],
Marek Wypych[1], Dawid Droździel[1], Artur Marchewka[1], Jarosław M. Michałowski[3],
Andreas Olsson[4], Ewelina Knapska[2]

[1] Laboratory of Brain Imaging, Nencki Institute of Experimental Biology of Polish Academy of Sciences, 3 Pasteur Str., 02-093 Warsaw, Poland

[2] Laboratory of Emotions Neurobiology, BRAINCITY - Centre of Excellence for Neural Plasticity and Brain Disorders, Nencki Institute of Experimental Biology of Polish Academy of Sciences, 3 Pasteur Str., 02-093 Warsaw, Poland

[3] Laboratory of Affective Neuroscience, SWPS University of Social Sciences and Humanities, 10 Kutrzeby Str., 61-719 Poznań, Poland

[4] Department of Clinical Neuroscience, Division of Psychology, Karolinska Institutet, Stockholm, Sweden

† These authors contributed equally to this work

Abstract

Humans often benefit from social cues when learning about the world. For instance, learning about threats from others can save the individual from dangerous first-hand experiences. Familiarity is believed to increase the effectiveness of social learning, but it is not clear whether it plays a role in learning about threats. Using functional magnetic resonance imaging, we undertook a naturalistic approach and investigated whether there was a difference between observational fear learning from friends and strangers. Participants (observers) witnessed either their friends or strangers (demonstrators) receiving aversive (shock) stimuli paired with colored squares (observational learning stage). Subsequently, participants watched the same squares, but without receiving any shocks (direct-expression stage). We observed a similar pattern of brain activity in both groups of observers. Regions related to threat responses (amygdala, anterior insula, anterior cingulate cortex) and social perception (fusiform gyrus, posterior superior temporal sulcus) were activated during the observational phase, reflecting the fear contagion process. The anterior insula and anterior cingulate cortex were also activated during the subsequent stage, indicating the expression of learned threat. Because there were no differences between participants observing friends and strangers, we argue that social threat learning is independent of the level of familiarity with the demonstrator.

Introduction

Detecting potential threats in the environment is vital for survival. To learn about danger, social species, including humans, use direct and vicarious cues (Olsson et al., 2020). Using vicarious cues is beneficial from the evolutionary perspective as it might eliminate the risk of first-hand encounters with a threat. One of the mechanisms underlying vicarious learning about dangers is emotional contagion, an automatic, unconscious tuning into the affective state of others. Due to such emotional mimicry, the observers can 'feel' the threat while enjoying relative safety themselves. Through exposure to the observed danger, they can learn about the potential risks within the environment.

The strength of the relationship between the 'demonstrator' and the 'observer' is believed to modulate emotional contagion (Preston & de Waal, 2002). In general, familiarity improves the social transfer of emotions (Bruder et al., 2012; de Vignemont & Singer, 2006; Gonzalez-Liencres et al., 2014; Hatfield et al., 2014). Importantly, however, previous research suggests that a close social relationship does not facilitate the emotional convergence of fear (Bruder et al., 2012). The only previous report comparing the neural correlates of a threat (an electric shock) to self, a friend, and a stranger gave no conclusive results (Beckes et al., 2013). Thus, it is unclear whether there is a difference between observational fear learning from friends and strangers.

To address this open question, we used a modified observational fear learning protocol (Haaker, Golkar, et al., 2017) improved in terms of ecological validity (Szczepanik, Kaźmierowska, et al., 2020). We directly tested how the demonstrator's familiarity influenced both psychophysiological and brain correlates of observational fear learning in the observer. The experimental design (Figure 1) involved two main stages. During the observational learning stage, two groups of participants (observers) witnessed their friends or strangers (demonstrators) undergoing a differential fear conditioning procedure. In this task, uncomfortable but not painful electric shocks were applied to the demonstrator's forearm during the presentation of emotionally neutral visual stimuli. Subsequently, during the direct-

expression stage, we tested the observers' brain responses to previously watched stimuli. No electrical stimulation was applied to the observers throughout the whole experiment. Thus, the observers derived the knowledge about the aversive value of stimuli only from social learning. As we wanted our experimental situation to be as naturalistic as possible, no apparent ingroup-outgroup division was introduced (we did not emphasize the demonstrator's affiliation). Also, unlike most previous studies that have used an actor serving as the demonstrator, real-time videos were transmitted to the observers in the friend-observation condition. In the stranger-observation condition, we used recordings from the friend-observation condition. Developing such an ecologically valid paradigm enabled investigating social learning of fear in a setting relevant for naturally occurring behaviors.

Figure 1

Experimental Design

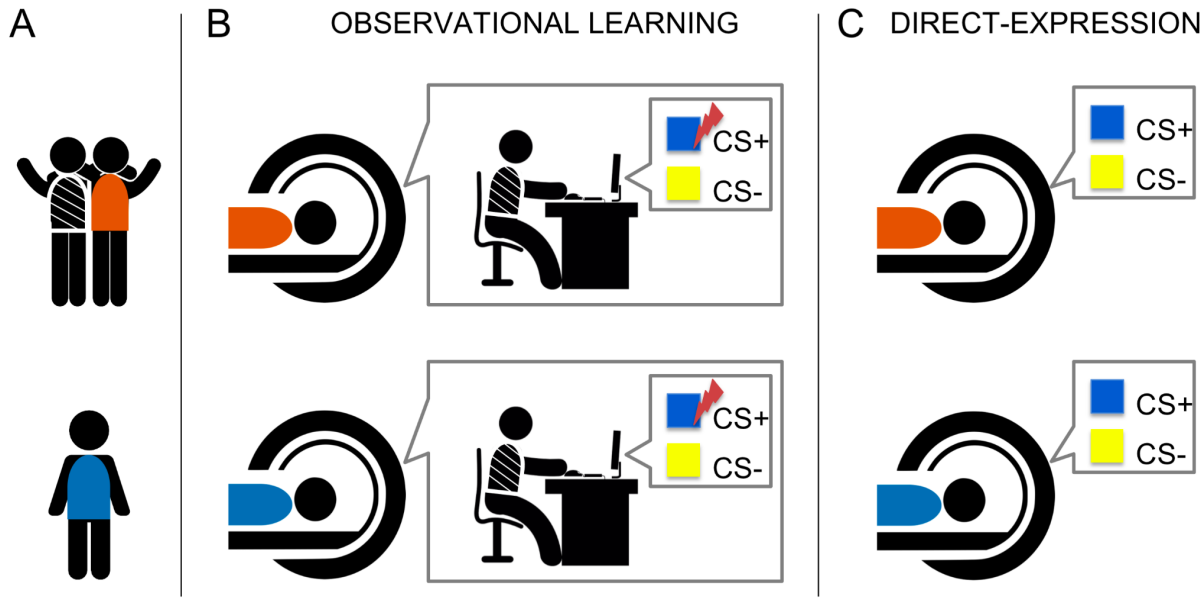

Note. (A) Depending on the group, observers arrived at the laboratory with their friend (upper panel, the 'friend' group, orange) or alone (lower panel, the 'stranger' group, blue). (B) During the observational learning stage, observers were lying in the fMRI scanner and watching the demonstrator (a friend or a stranger) performing the differential fear conditioning task. In the task, one stimulus (conditioned stimulus +; CS+) was sometimes paired with an uncomfortable

electric shock (unconditioned stimulus, US), while the other one (conditioned stimulus -; CS-) was always safe. (C) During the direct-expression stage, observers remained in the scanner and were told that they would perform the same task as previously watched. They watched an identical set of visual stimuli, but no electrical stimulation was applied.

Results

Behavioral Results

Stimulus Contingency Awareness

After completing both stages of the experiment, the observers answered a set of questions about the relationship between the electrical stimulation and the visual cues in the observational learning stage (see Assessment of Stimulus Contingency Knowledge). 35 out of 48 participants in the friend group and 35 out of 44 participants in the stranger group correctly identified the CS+/US contingency. The proportion of contingency-aware and non-aware participants was not significantly different between groups (chi-squared = 0.554, df = 1, p = 0.46). We included only the contingency-aware participants in further analyses (Szczepanik, Kaźmierowska, et al., 2020).

Evaluation of the Demonstrator's Expression (the Observational US)

Next, the observers evaluated the demonstrator's expression (the observational US) by answering a set of questions scored on 0 - 9 scales. The questions concerned the demonstrator's reactions to electrical stimulation (how much discomfort they experienced, how expressive they were, and how natural their reactions were) and their attitude (how much empathy they felt for the demonstrator). Additionally, in the pairs of friends, the observers assessed how well they could identify with the demonstrator. Median ratings in both the friend and stranger groups were between 5 and 7 (see Figure 2). Additionally, we asked the observers to rate the degree of unpleasantness attributed to the demonstrators on a 1 - 5 scale (from very unpleasant to very pleasant). The median ratings were between 1 (very unpleasant)

and 2 (rather unpleasant). The Wilcoxon-Mann-Whitney test showed no significant differences between the groups in any category. See Table S1 in the Appendix for detailed statistics.

Figure 2

Evaluation of the Demonstrator's Expression (the Observational US)

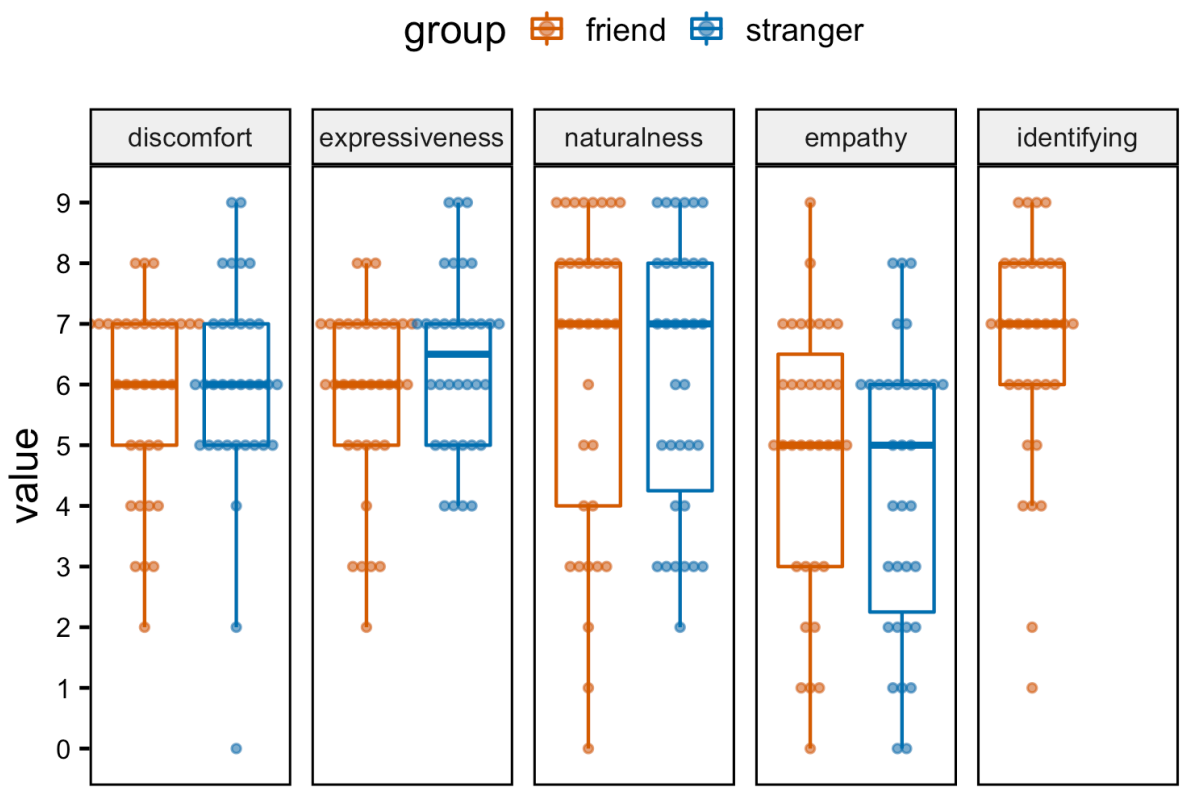

Note. Error bars extend to data points placed no further than 1.5*IQR (interquartile range) beyond the 1st quartile and above the 3rd quartile.

Empathy and Anxiety - Questionnaire Results

The state anxiety was tested twice, before and after the experiment. The results were analyzed for the contingency-aware observers, who were included into the fMRI analysis. Repeated-measures ANOVA and analogous Bayesian repeated measures ANOVA with the group (friend, stranger) as a between-subject factor and measurement (before, after) as a within-subject factor showed no significant differences: main effect of the group: $F(1, 67) = 0.76$, $\eta_g^2 = .009$, $p = .39$, $BF_{incl} = 0.35$; main effect of the measurement: $F(1,67) = 1.92$, $\eta_g^2 =$

.007, p = .17, BF_{incl} = 0.36; group × measurement interaction F(1,67) = 1.29, η_g^2 = .004, p = .259, BF_{incl} = 0.14.

The trait anxiety index, and three subscales of the empathic sensitiveness scale were treated independently, and compared between friend- and stranger-observers groups using two sample t-tests. Again, none of the comparisons was statistically significant and indicated either absence of evidence or moderate evidence against the difference: trait anxiety: t = 1.07, df = 63.5, p = 0.29, BF = 0.40; empathic concern: t = 0.20, df = 59.0, p = 0.85, BF = 0.25; personal distress t = 1.11, df = 64.1, p = 0.27, BF = 0.42; perspective taking: t = 0.12, df = 63.2, p = 0.91, BF = 0.25.

Skin Conductance Responses

Amplitudes of the observers' skin conductance responses (SCR) were compared (separately for each stage of the experiment) using classical and Bayesian repeated measures ANOVA, with group (friend, stranger) as a between subjects factor. In the observational learning stage, ANOVA revealed a significant main effect of the stimulus (US / no US), F(1, 52) = 29.19, η_g^2 = .089, p < .001, BF_{incl} = 6976 where participants showed stronger reactions to the US compared to no US, t(52) = 5.40, p < .001, BF = 11341 (Figure 3 A). The main effect of the group, F(1,52) = 2.21, η_g^2 = .034, p = .14, BF_{incl} = 0.75, and the stimulus × group interaction, F(1,52) = 0.55, η_g^2 = .002, p = .46, BF_{incl} = 0.63, were not significant. Similarly, in the direct-expression stage, we found a significant effect of the stimulus (CS+/CS-), F(1, 52) = 5.73, η_g^2 = .018, p = .02, BF_{incl} = 1.79, with stronger reactions to CS+ than CS-, t(52) = 2.39, p = .02 , BF = 2.02 (Figure 3 B), while the main effect of the group, F(1, 52) = 1.89, η_g^2 = .029, p = .18, BF_{incl} = 0.62, and the stimulus × group interaction, F(1,52) = 0.83, η_g^2 = .003, p = .37, BF_{incl} = 0.464, were not significant.

Figure 3

Skin Conductance Responses

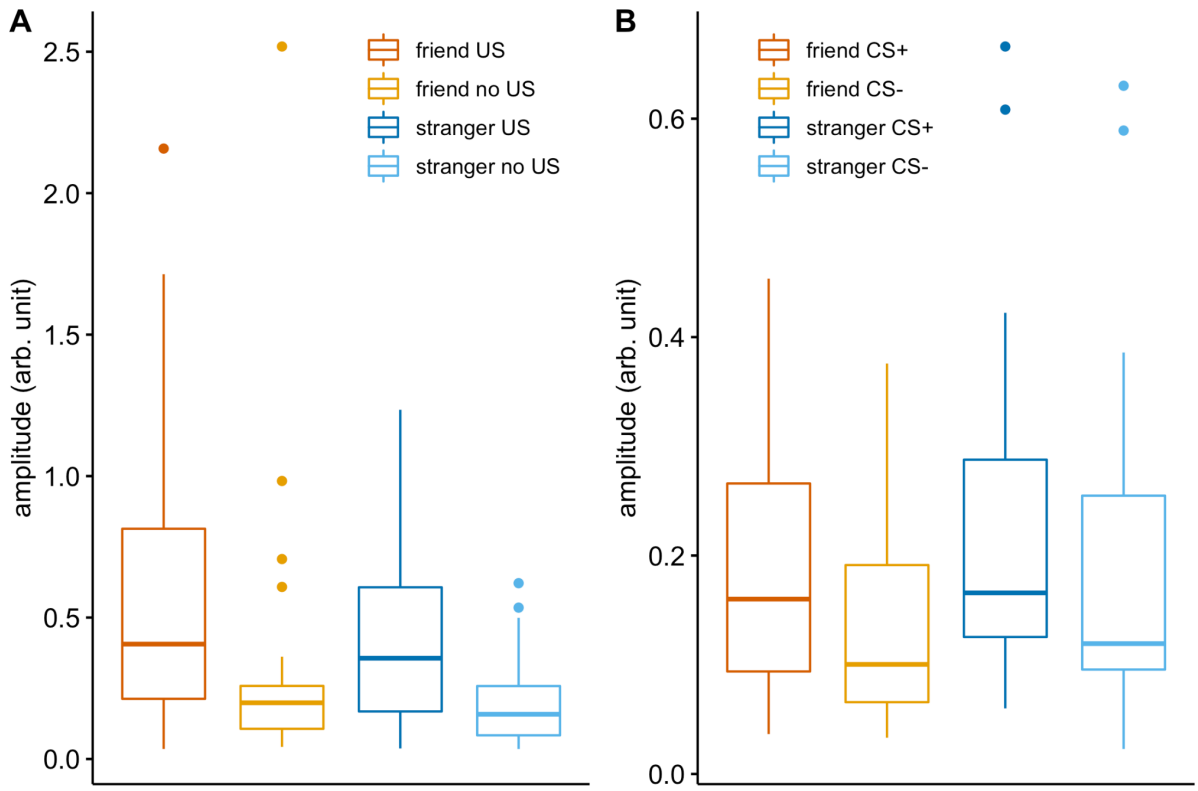

Note. (A) observational learning stage, (B) direct-expression stage. Error bars extend to data points placed no further than 1.5*IQR beyond the 1st quartile and above the 3rd quartile.

Imaging Results

Brain Activation Analysis - Observational Learning Stage

In the observational learning stage, we analyzed the whole-brain activity of the observers witnessing the demonstrator's reaction to the aversive stimulation. We compared it to the corresponding periods when the CS appeared without aversive stimulus (US > no US). To test the main effect of the task, we first evaluated the US > no US contrast for both groups. It revealed a robust and extensive activation ($p < 0.05$, FWE peak-level correction) of multiple brain regions, including the bilateral amygdala, bilateral anterior insula (AI), and anterior mid-cingulate cortex (aMCC), the bilateral posterior superior temporal sulcus (pSTS) and bilateral fusiform gyrus, including the fusiform face area (FFA).

Next, we compared the friend and stranger groups directly, i.e., with the (friend US > no US) vs. (stranger US > no US) using t contrasts (see Figure 4 A). The whole-brain analysis yielded no significant between-group differences (with either peak- or cluster-level FWE

corrections). To further compare the groups, we performed region-of-interest analysis (averaging parameter estimates within a region) for the six pre-selected areas, defined independently of the functional data (AI, aMCC, amygdala, FFA, rpSTS, rTPJ). We found no significant differences between the friend and stranger groups; Bayes Factor analysis indicated moderate evidence for the absence of effects ($BF_{01} > 3$) in all regions except the rTPJ, where the evidence was inconclusive ($BF_{01} = 2.07$), see Table 1 and Figure 4 B.

An additional between-group comparison, based on the observational US reactions, i.e., friend US > stranger US t contrast, also did not yield significant differences on a whole-brain level. Region-of-interest analysis for this contrast (using the same set of regions as above) confirmed the lack of significant between-group differences. At the same time, Bayes factors indicated evidence that was either inconclusive or moderately favored the null hypothesis (all BF_{01} between 1.36 and 4.04), see Table 1 and Figure 4 - figure supplement 1.

Figure 4

Activation in the Observational Learning Stage, US > no US Contrast

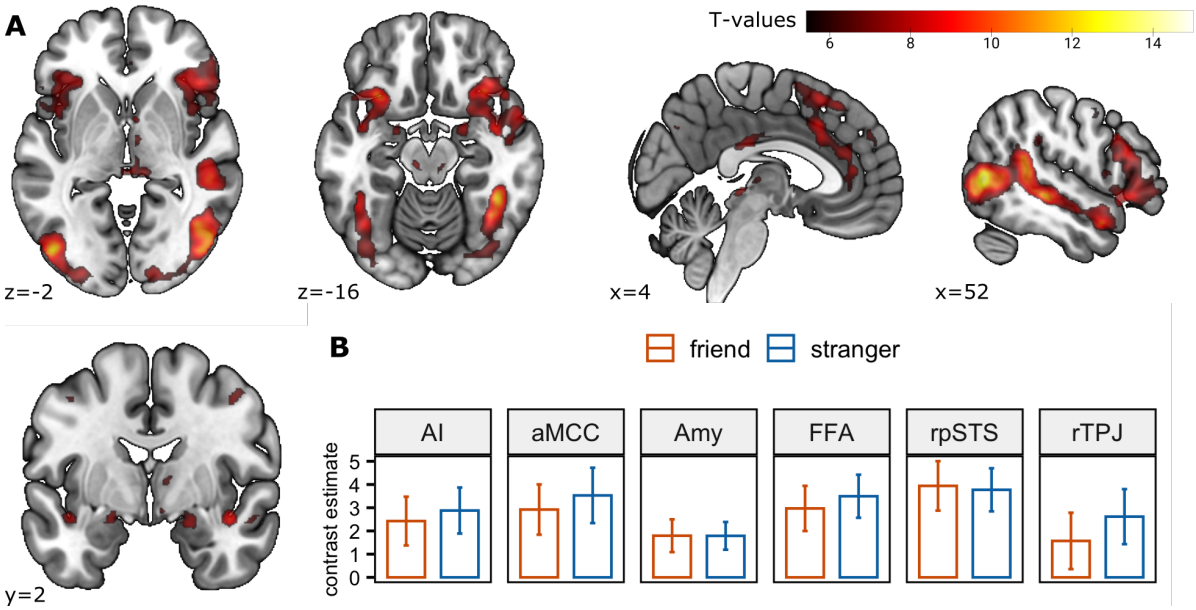

Note. We found no between-group differences. (A) Statistical maps show whole-brain activations for both groups analyzed together, $p < 0.05$, FWE peak-level correction. (B) Region-

209 of-interest statistics, showing group averages and 95% confidence intervals. Abbreviations: AI
210 - anterior insula, aMCC - anterior mid-cingulate cortex, Amy - amygdala, FFA - fusiform face
211 area, rpSTS - right posterior superior temporal sulcus, rTPJ - right temporo-parietal junction.
212
213 **Figure 4 - figure supplement 1**
214 *Region-of-interest Statistics for the Observational Learning Stage*

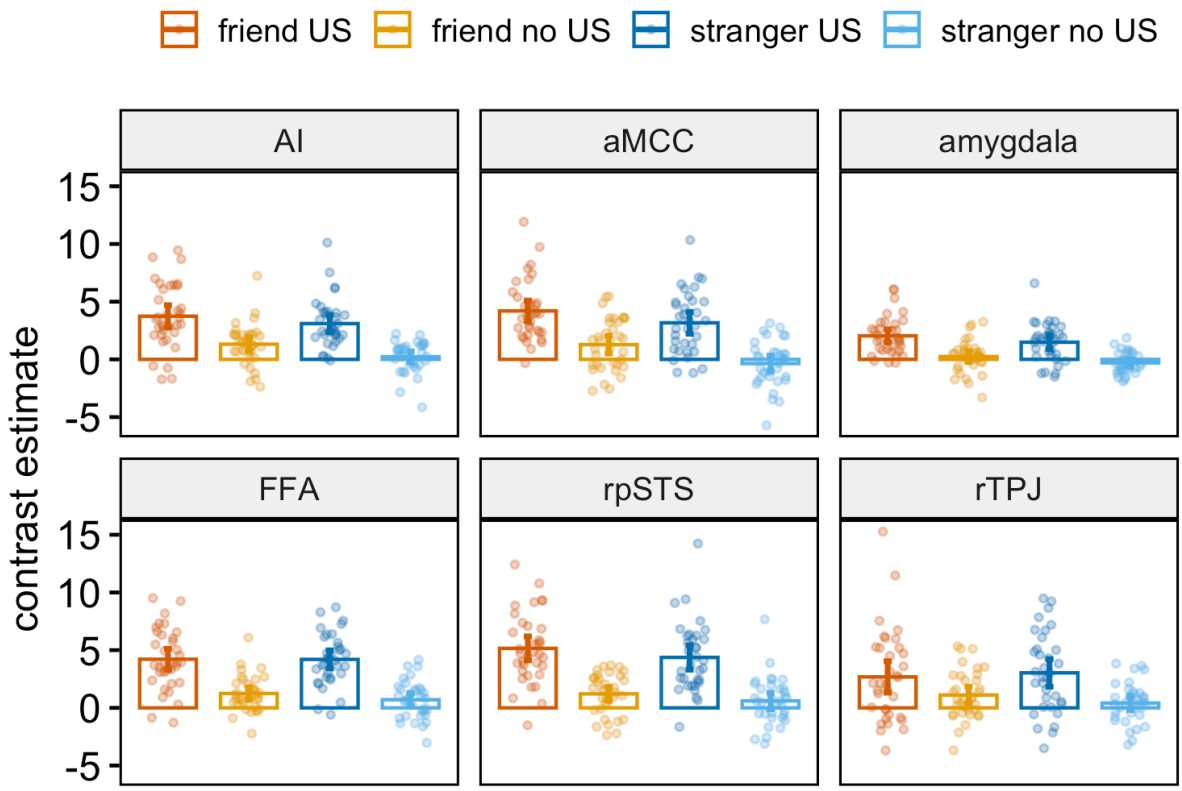

215
216 *Note.* Parameter estimates (group average and 95% confidence intervals, with subjects
217 represented by dots) are shown for the US and no US separately. AI - anterior insula, aMCC -
218 anterior mid-cingulate cortex, FFA - fusiform face area, rpSTS - right posterior superior
219 temporal sulcus, rTPJ - right temporo-parietal junction.
220
221 ***Brain Activation Analysis - Direct-expression Stage***
222 To measure observational fear learning, i.e., the association formed between the CS
223 and the observational US, in the direct-expression stage, we analyzed the brain activity of the
224 observers in response to the conditioned stimuli (CS+ > CS-). To evaluate the main effect of

the task, the CS+ > CS- contrast was first analyzed for both groups together and subsequently compared between the groups.

Analyzing both groups together, we observed significant activations in the bilateral AI and the aMCC (Figure 5). Next, we performed a direct between-group comparison, i.e., friend (CS+ > CS-) vs. stranger (CS+ > CS-), which yielded no significant differences on the whole-brain level. We performed a region-of-interest analysis with the same set of regions as in the observational learning stage to further compare the groups. We found no significant differences, and Bayes Factor analysis indicated moderate evidence for the absence of effects (BF_{01} > 3) in all regions except the rpSTS where the evidence was inconclusive (BF_{01} = 2.32); see Table 1 and Figure 7.

Figure 5

Activation in the Direct-expression Stage, CS+ > CS- Contrast

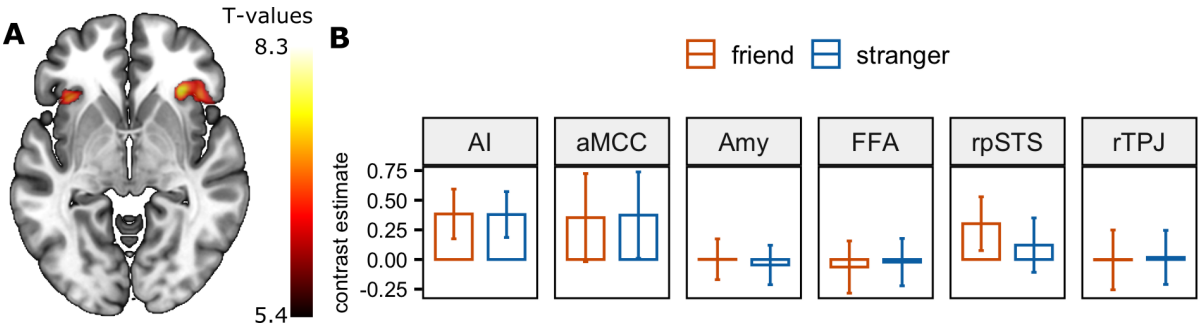

Note. (A) Statistical map showing whole-brain activations for the friend and stranger groups analyzed together, FWE corrected, p < 0.05. (B) Region-of-interest statistics, showing group averages and 95% confidence intervals. Abbreviations: AI - anterior insula, aMCC - anterior mid-cingulate cortex, Amy - amygdala, FFA - fusiform face area, rpSTS - right posterior superior temporal sulcus, rTPJ - right temporo-parietal junction.

To capture the potential effects of extinction during the direct-expression stage, we included 1st order temporal modulation in the statistical model. Analyzing both groups together, we observed a significant decrease in the brain responses to CS+ across several

regions, most notably in the aMCC. To test whether the groups differed concerning the temporal dynamics of brain responses, we evaluated the (friend CS+ × t) vs. (stranger CS+ x t) contrast. We observed the differences in some brain regions, including the left inferior frontal gyrus, left middle temporal gyrus, right lingual gyrus, and left putamen. Strangers showed a stronger linear decrease in activity than friends (see Figure 6 and Table S5). Importantly, however, we found no differences in the structures activated in the observational and direct-expression stages.

Figure 6

Temporal Modulation of the CS+ Response in the Direct-expression Stage

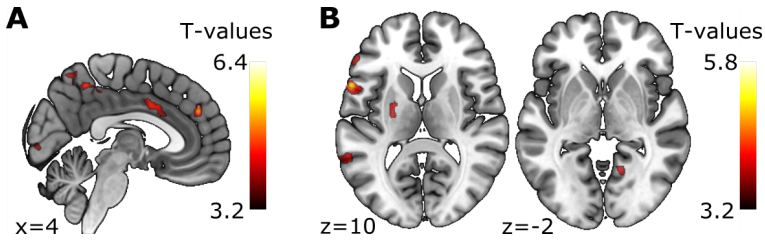

Note. (A) Statistical map showing a significant effect for the friend and stranger groups analyzed together. (B) Statistical map showing the (stranger CS+ × time decrease) > (friend CS+ × time decrease) contrast.

Table 1

Region-of-interest Analysis of Between-group Differences

ROI	Observational Learning Stage (US > noUS)			Observational Learning Stage (US)			Direct-expression Stage (CS+ > CS-)		
	t	p	BF_{01}	t	p	BF_{01}	t	p	BF_{01}
AI	-0.64	.52	3.39	1.06	.29	2.50	0.03	.97	4.04
aMCC	-0.77	.45	3.13	1.60	.11	1.36	-0.08	.93	4.03

Amy	0.01	.99	4.04	1.38	.17	1.79	0.40	.68	3.76
FFA	-0.80	.43	3.08	0.03	.98	4.04	-0.28	.78	3.90
rpSTS	0.24	.81	3.94	1.08	.29	2.47	1.14	.26	2.32
rTPJ	-1.25	.21	2.07	-0.49	.69	3.78	-0.13	.90	4.01

Note. We performed two comparisons for the observational learning stage based on within-subject parameter estimates for either the (US > no US) or the US alone. We compared the (CS+ > CS-) contrast estimate between the groups for the direct-expression stage. The statistical results: positive t values represent friend > stranger; t-tests with Welch correction to the degrees of freedom; p values not corrected for the number of comparisons; Bayes factors reported in favor of the null hypothesis. AI - anterior insula, aMCC - anterior mid-cingulate cortex, Amy - amygdala, FFA - fusiform face area, rpSTS - right posterior superior temporal sulcus, rTPJ - right temporo-parietal junction.

Psychophysiological Interactions

We performed a psychophysiological interaction (PPI) analysis for several selected ROIs to investigate the coupling between the activated structures. First, we analyzed the observational learning stage, focusing on the US > no US contrast. As the seed structures, we used the AI, rpSTS, aMCC, amygdala, FFA, and rTPJ. Analyzing both groups together, we observed increased coupling of the AI with several regions, including the rpSTS (Figure 7 A), and stronger coupling of the rpSTS with the AI, right fusiform gyrus (Figure 7 B), and amygdala (Figure 7 C). However, there were no significant differences between the groups. Similarly, we did not find the group differences using the aMCC, amygdala, FFA, and rTPJ as the seed structures. Further, we applied the PPI analysis to the activations observed during the direct-expression stage, using the AI, aMCC, and amygdala as the seeds. We did not find significant differences for the groups analyzed together or between the friend and stranger groups.

Figure 7

Psychophysiological Interaction Maps, US > no US Contrast

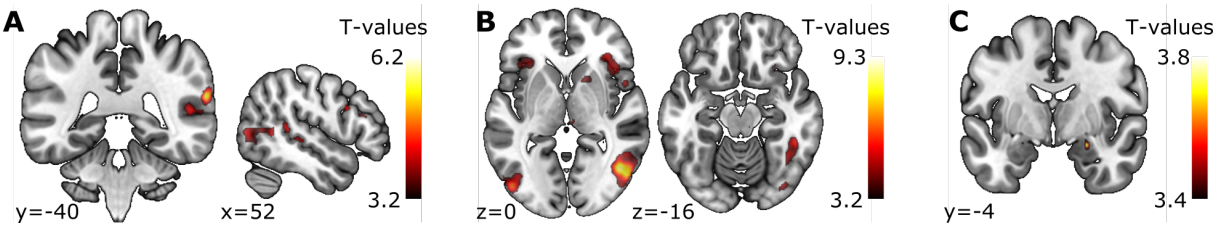

Note. AI and pSTS seeds were analyzed for both groups together during the observational learning stage. (A) the AI exhibits interaction with several regions, including the rpSTS (FWEc), (B) the rpSTS exhibits interaction with several areas, including the right fusiform gyrus and bilateral AI (FWEc), (C) psychophysiological interaction of the rpSTS with the amygdala (SVC).

Discussion

Here, we investigated the relevance of the demonstrator's familiarity in observational fear learning using physiological and neural measures. We focused on the US > no US contrast in the observational learning and the CS+ > CS- contrast in the direct-expression stage. We found no significant differences between participants observing friends ('friend' group) and subjects watching strangers ('stranger' group), neither in fear contagion nor in observational fear learning. Our study is the first to directly examine the difference between neural correlates of observational fear learning from friends and strangers. Using the ecologically valid paradigm that has been developed and tailored for this study, we replicated the previously reported brain activations underlying fear conditioning in humans. However, brain activity did not differ between participants observing friends and strangers. This clarifies the role of familiarity in fear contagion in humans and is in line with the previous rodent reports (Hernandez-Lallement et al., 2020). Overall, our results show that humans learn fear equally from friends and strangers, which might have been evolutionarily beneficial.

Main Physiological and fMRI Effects - Validation of the Protocol

We improved the original protocol of Haaker, Golkar et al. (2017) to study a real-time demonstrator-observer interaction. To validate the modified protocol, we firstly examined the data regardless of the level of familiarity. We analyzed both physiological and neural correlates of observational fear learning. The majority of observers correctly identified the CS+/US contingency and the contingency-aware to non-aware participants ratio, around three-quarters, was similar across groups. As our previous study showed that the psychophysiological effects of observational fear learning were present only in the contingency-aware participants (Szczepanik, Kaźmierowska, et al., 2020), we included only those in the analyses.

We observed enhanced observers' skin conductance response (SCR) to the shock-associated stimuli during both observational learning and direct-expression stages, which is in line with earlier reports (Sevenster et al., 2014; Szczepanik, Kaźmierowska, et al., 2020). Neuroimaging analysis of data collected during the observational fear learning stage (US > no US contrast) revealed brain activity in multiple regions, including those crucial for fear-related processing (amygdala, AI, aMCC), which is consistent with previous studies (Lindström et al., 2018). Additionally, we observed activation of brain areas involved in dynamic social perception (fusiform gyrus, pSTS, and supplementary motor area), which may indicate processing of visual body cues (Allison et al., 2000; Yang et al., 2015). PPI analysis revealed coupling of the AI with the rpSTS and of the rpSTS with the AI, right fusiform gyrus, and amygdala, suggesting that these brain regions are jointly involved in the social transfer of fear. Brain activity during the direct-expression stage (CS+ > CS- contrast) involved the bilateral insular cortex and aMCC, which is in line with previous findings (Lindström et al., 2018; Olsson et al., 2007). We did not observe significant amygdala activations. In the direct fear conditioning, the amygdala is considered a region where the CS-US association is stored (Olsson & Phelps, 2007; Phelps & LeDoux, 2005). However, none of the previous studies has provided consistent evidence for the amygdala involvement during the direct-expression stage. Additionally, a meta-analysis on the neural signatures of the human fear conditioning has shown that the amygdala is not reliably activated when fMRI fear conditioning tasks are

345 employed (Fullana et al., 2016). Taken together, using the ecologically valid paradigm, we
346 replicated most of the previously reported brain activations underlying fear conditioning in
347 humans.
348
349 **Familiarity Effects**
350 We employed the experimental design in which familiarity with the demonstrator was
351 the only between-group difference. We also made sure that the observers learned about the
352 threat through social means only - they did not directly experience any electrical stimulation at
353 any point of the experiment. The questionnaire results indicated that the observers from both
354 groups did not differ in their general level of anxiety and empathy-related traits. Also, their initial
355 state of anxiety (measured at the beginning of the experiment) was similar. Notably, the
356 expressions of the demonstrators (the observational US) were rated as natural and did not
357 differ between the groups. This lack of differences indicates that the experimental conditions
358 were similar across groups, which is essential considering the naturalistic paradigm employed
359 and potential confounds related to individual differences in the demonstrators' fear expression.
360 We found no significant differences in the brain activations of observers learning about
361 the threat from their friends or strangers. The only previous report directly comparing the neural
362 correlates of threat-to-self, threat-to-friend, and threat-to-stranger experience (Beckes et al.,
363 2013) used a within-subject design. The within-subject protocol makes it difficult to disentangle
364 the impact of direct vs. social sources of information. Our results show that familiarity between
365 the participants does not modulate social fear learning when a demonstrator is a sole source
366 of information.
367 In contrast to our results, the social learning of pain activated the pain network
368 components (ACC and AI) depending on whether the participants imagined a loved one or a
369 stranger (Cheng et al., 2010). This result seems to be at odds with our findings. However, the
370 fear and pain paradigms differ. Although both paradigms use aversive stimulation (often
371 involving electric shocks), the former emphasizes that it should be uncomfortable but not
372 painful. In our study, we adjusted the electric shock's intensity by asking every demonstrator

to choose the level of electric stimulation and instructing him to react ‘in a natural, yet noticeable manner’. Based on the observers’ post-experimental ratings (on average describing the degree of unpleasantness attributed to the demonstrators as ‘rather unpleasant’), we may suppose they did not interpret the demonstrators’ condition in terms of pain.

Animal studies provide somewhat disparate results on the role of familiarity in threat contagion (Gonzalez-Liencres et al., 2014; Jeon et al., 2010; Knapska et al., 2010; Sanders et al., 2013). The studies carried out in a well-known environment, in which the presence of a partner attenuates threat response (the effect known as social buffering (Kiyokawa et al., 2014)) more consistently report familiarity effect. Thus, familiarity may play a role in social attenuation rather than the social enhancement of fear. In line with this reasoning, a recent meta-analysis of rodent studies indicated no familiarity effect on emotional contagion of threat (Hernandez-Lallement et al., 2020). The lack of familiarity effect in threat contagion may stem from the fact that social learning about danger, especially in a novel environment, is equally effective and might have been evolutionary beneficial regardless of the demonstrator’s level of familiarity.

Emotional contagion is considered a primary form of empathy, which results from the basic mechanism of the Perception-Action Model (De Waal, 2012; de Waal & Preston, 2017). The PAM involves automatic matching between the target’s and the observer’s neural responses and constitutes a foundation for more complex phenomena such as sympathetic concern and perspective-taking. The model predicts that emotional contagion is more robust among individuals in close social relationships as their perception-action coupling is stronger (Preston & de Waal, 2002). However, our data show that fear contagion does not depend on the level of familiarity, which may stem from its crucial informative role. In the face of threat, observing the emotional responses of others can facilitate life-saving responses (Olsson et al., 2020). It is noteworthy that the actors serving as demonstrators in previous observational fear learning studies were all unfamiliar to the observers and still remained an effective source of learning (Golkar et al., 2015; Golkar & Olsson, 2017). Thus, perceiving the emotions of others not only provides information about their source, i.e., the emotional state of the ‘demonstrator’

but also about the environment. Friends and strangers are equally good as a source of information about threats.

Limitations

Since the participants came together to the laboratory in the ‘friend’ group, the situation was more natural and socially engaging than in the ‘stranger’ group, where the observers had no interaction with the demonstrators before the experiment. However, if this was an essential factor, we could expect stronger activations of the social brain network in the ‘friend’ group, which was not the case. Moreover, we did not directly measure observers’ empathy toward the demonstrators. However, we assessed observers’ general level of empathy, identification with a demonstrator, and degree of unpleasantness attributed to the demonstrator and did not find differences between the groups. Finally, we studied only males; thus, it is unclear whether the results extrapolate to the female population. Considering the sex differences in emotional processing and empathy (Proverbio, 2021) and a pioneering character of the study, limiting the probe to one sex only enabled us to watch relatively strong and statistically powered effects. However, this issue certainly requires future investigations.

Conclusion

We describe here the neural correlates of observational fear learning in humans using a naturalistic approach. Using this paradigm, we replicated most of the previously reported brain activation underlying fear conditioning in humans. Importantly, our findings constitute the first neuroimaging evidence for the lack of relationship between familiarity and fear contagion and observational fear learning in humans. We argue that fear contagion is an automatic, unconscious process independent of the level of the demonstrator’s familiarity. We claim that fear is learned equally from friends and strangers in humans, which is evolutionarily beneficial. These results resonate with ongoing debates on the questions such as the components of empathy, the boundaries between unconscious threat processing and conscious fear experience, and the role of the amygdala in the fear conditioning process. A question of the

429 demonstrator's characteristics modulating the observational fear learning process remains
430 open, creating a space for further investigations.
431
432 **Methods**
433
434 **Participants**
435 48 pairs of friends ('friend' group) and 47 individuals ('stranger' group) participated in
436 the experiment. Pairs of friends took part in the experiment together, with one participant being
437 a demonstrator and another an observer. The demonstrators undergoing fear conditioning
438 were live video streamed in the 'friend' group, and their video recordings were used in the
439 'stranger' group. Only the observers underwent fMRI. To estimate groups' sizes that provide
440 sufficient statistical power, we considered a similar fMRI experiment with the between-group
441 design (n=21 and n=22 (Haaker et al., 2017)). We increased the number of recruited
442 individuals as the rate of contingency-aware participants is lower in a real-time demonstrator-
443 observer interaction (Szczepanik, Kaźmierowska, et al., 2020). The eligibility criteria included
444 being heterosexual male, aged between 18 and 30 years, right-handed, and native or fluent
445 Polish speaker. We excluded students and graduates of either psychology or cognitive
446 science, participants with neurological disorders or other medical conditions precluding MR
447 scanning or electrical stimulation, and participants taking psychoactive drugs. Additionally, in
448 the 'friend' group, the participants had to have known each other for at least three years and
449 score at least 30 out of 60 points in the McGill Friendship Questionnaire - Respondent's
450 Affection, see Behavioral Measures.
451 We excluded four subjects from the 'stranger' group: three subjects who experienced
452 technical problems with the video playback, and one subject who showed excessive head
453 motion during one of the tasks (more than 25% volumes classified as motion outliers, see fMRI
454 Data Preprocessing section). We included only the contingency-aware participants in the
455 analyses; please refer to Assessment of Stimulus Contingency Awareness (Szczepanik,
456 Kaźmierowska, et al., 2020). The final group sizes were n = 35 ('friend' group) and n = 34

('stranger' group). In the analyzed sample, the mean age of all observers was 22.9 years (SD = 2.87), the mean length of the observer-demonstrator friendship was 7.7 years (SD = 4.22), and the mean observers' score in the McGill Friendship Questionnaire was 52 (SD = 7.74), see Table S2 in Appendix for the detailed statistics. All participants received financial remuneration of 100 PLN (~23 EUR) for their participation.

Tasks and Stimuli

Experimental Setup

In the MRI scanner, the observer watched a video (either a streaming or a replay, both without sound) or picture stimuli on an MR-compatible monitor through a mirror box placed on the head coil. The demonstrator sat in a small room adjacent to the MR room (in the 'friend' group). A GoPro Hero7 camera provided video transmission and recording. To ensure reliable reproduction of stimuli' colors, we lighted the room with an LCD panel with adjustable color temperature, set the computer screen brightness to low, and adjusted the camera's white balance. The room walls were covered with gray acoustic foam to minimize distractors.

Stimuli

The conditioned stimuli were two squares, blue and yellow, displayed on a gray background. The squares were presented centrally and covered either a half (during the observation stage) or a quarter (during the direct-expression stage) of screen height (Figure 8). The assignment of color to CS+ and CS- was counterbalanced across participants.

Cutaneous electrical stimulation, applied to the ventral part of a forearm of the demonstrator, was used as the unconditioned stimulus. Stimulating electrodes were placed above the *flexor carpi radialis* muscle so that even low-intensity stimulation caused involuntary muscle flexion, visible to the observer. The stimulation consisted of five unipolar pulses of 1 ms duration applied in 200 ms intervals. The demonstrators individually adjusted shock intensity to be unpleasant but not painful (see Demonstrator's Preparation and Instructions).

Observational Learning Stage

The observer watched the demonstrator performing a differential conditioning task. The demonstrator watched 24 CS+, and 24 CS- displayed on the screen in pseudo-random order, with a given CS repeated at most twice in a row. Each CS lasted 9 seconds, half of the CS+ reinforced with the US. The US reinforced the first and the last presentation of CS+. The US started 7.5 seconds after the CS onset to allow the demonstrator's reaction to co-terminate with the CS. The CS- was never reinforced. The intertrial intervals (ITIs) lasted randomly between 10 and 15 seconds, with a fixation symbol (+) displayed centrally on the screen (Figure 8).

Direct-expression Stage

The observer watched 12 CS+ and 12 CS-. The stimuli and the stimuli' order, timing, and ITI were the same as during the observational learning stage. None of the CS was reinforced.

Figure 8

Tasks and Stimuli Overview

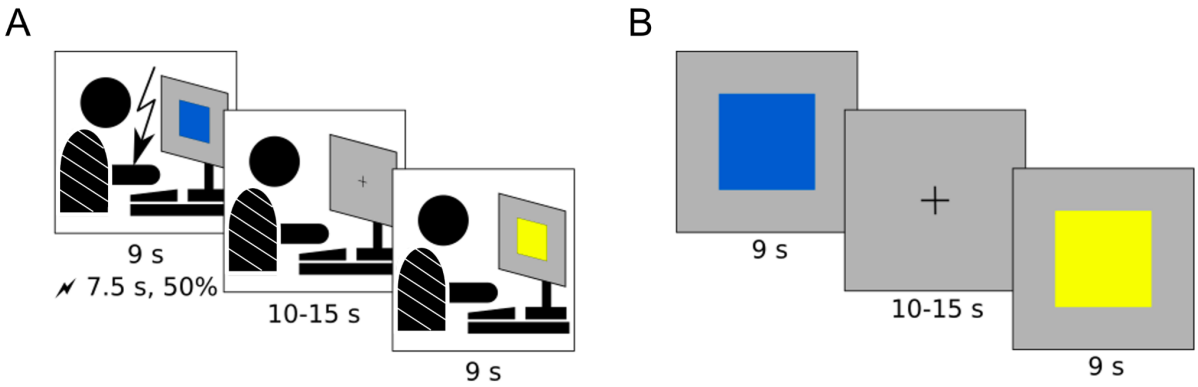

Note. Schematic representation of the task design. (A) The observational learning stage: participants watched another person (demonstrator) who performed a differential conditioning task. The US (electrical stimulation) reinforced half of the visual CS+, CS- were never reinforced. (B) The direct-expression stage: participants, informed that they would undergo an

identical task as the demonstrators, watched the same visual stimuli presentation. However, the electric stimulation was not applied.

Procedure

To investigate observational fear learning, we adapted the protocol of Haaker, Golkar, et al. (2017) for live observation of demonstrator-observer interaction (Szczepanik, Kaźmierowska, et al., 2020). The protocol was approved by the Ethics Committee of the Faculty of Psychology at the University of Warsaw (decision from 28 November 2017). The procedure complied with the Ethical Principles of Psychologists and Code of Conduct published by the Polish and the American Psychological Associations.

Before the Experiment

The participants received brief information about the experimental procedure, including the possibility of receiving aversive electrical stimulation. Next, the participants gave informed consent (including optional permission for recording and recording's reuse) and filled in safety screening forms. The roles of a demonstrator and an observer were then randomly assigned to the participants by giving two color-coded envelopes. Then the participants were isolated; the demonstrators went to a room adjacent to the MR room.

Observer's Preparation and Instructions

First, the observers filled in the questionnaires (see Behavioral Measures for details). Next, they opened the envelope with the role assignment and received instructions. The instruction included information on the two-stages procedure in the fMRI scanner. The instruction said that, firstly, the participants would watch their friends perform a task involving the presentation of colored symbols and the administration of unpleasant electrical stimulation. Then, they would perform an identical task themselves. Importantly, no information about the stimuli contingency was provided. After receiving the instruction, the observers had stimulation and skin conductance electrodes attached and went to the MR room. In the scanner, the

subjects had sham leads connected to the stimulation electrodes attached to make receiving electrical stimulation believable.

Demonstrator's Preparation and Instructions

First, the demonstrators filled in the questionnaires (see Behavioral Measures for details). Next, they opened the envelope with the role assignment and received instructions. The instruction said they would perform a task involving the presentation of colored symbols and administering unpleasant, but not painful, electrical stimulation. Unlike the observers, the demonstrators received information on the stimuli contingency and reinforcement rules. We asked the demonstrators to react to the stimulation in a natural yet noticeable manner. The demonstrators watched a recording with a model reaction. After receiving the instruction, the demonstrators had stimulation and sham skin conductance electrodes attached. Afterward, the demonstrators adjusted stimulation intensity. The experimenter increased it stepwise, and the participants rated the intensity using a scale from 1 (*imperceptible*) to 8 (*painful*). The target level was 6 (*very unpleasant but not painful*).

MRI Procedure

The MRI scanning started with the acquisition of an anatomical image. Then, the observational learning stage followed (see Tasks and Stimuli). The experimenter adjusted the camera's position to ensure that the observer could see the demonstrator's face, hand, and computer screen and turned on video transmission and recording. The observer received a brief reminder: 'in this part of the study, you will observe your friend performing a certain task'. After completion of the observational learning stage, the observer received a brief reminder: 'in this part of the study, you will perform the same task that you just watched', and the direct-expression stage ensued (see Tasks and Stimuli).

Conclusion of the Experiment

While the observer took part in the direct-expression stage, the demonstrator completed the post-experimental questionnaires (see Behavioral Measures for details). After the MRI session ended, the observer also completed their set of post-experimental questionnaires, and both participants were debriefed about the study.

Stranger Group

In the 'stranger' group, only one subject (the observer) participated in the experimental session. Instead of a live stream, we used 45 recordings made in the 'friend' group. Otherwise, the procedure in the stranger group was very similar to that involving a pair of friends and differed only in the necessary aspects. There was no role assignment, and instructions given to the observers referred to another person rather than a friend.

Behavioral Measures

McGill Friendship Questionnaire - Respondent's Affection

To recruit pairs of friends, we used the McGill Friendship Questionnaire - Respondent's Affection (Mendelson & Aboud, 1999); translated by A. Kaźmierowska, P. Pączek, and A. Schudy for online screening in this study. It consists of 16 positive statements describing feelings for a friend and satisfaction with the friendship, rated along a 9-point scale ranging from -4 (*very much disagree*) to 4 (*very much agree*). One item (no. 9) was omitted from the questionnaire due to human error. A score of 30 points was a threshold for inclusion in the study.

Empathic Sensitiveness Scale

To measure the participants' empathy, we used the Empathic Sensitiveness Scale (original title: Skala Wrażliwości Empatycznej, SWE (Kaźmierczak et al., 2007)). It is a self-report questionnaire based on the Interpersonal Reactivity Index (Davis, 1983), but with far-reaching modifications developed in the Polish language. It contains 28 statements, which

reflect three components of empathy: two emotional (empathic concern, personal distress) and one cognitive (perspective taking). The answers are given on a 5-point scale. The demonstrators and observers filled in the questionnaire at the end of the experimental procedure.

State and Trait Anxiety Inventory

To measure participants' anxiety, we used the State and Trait Anxiety Inventory (Spielberger et al., 1983, polish adaptation 2012). It is a self-report questionnaire consisting of two 20-item subscales, STAI-State and STAI-Trait. Participants rate statements related to how they feel either at a given moment (state) or usually (trait) using 4-point Likert scales. Each participant completed the STAI-state twice (at the beginning and the end of the experiment) and STAI-trait once (at the end of the experiment).

Assessment of Stimulus Contingency Awareness

To assess the observers' declarative knowledge of the CS/US contingency, we used an online questionnaire adapted from (Weidemann et al., 2016). The questionnaire referred to the observational learning stage and was divided into several parts to eliminate guessing. Firstly, it asked whether the participant could predict shocks to the demonstrator. Then, if answered positively, an open-ended question 'how' followed. Next, participants gave percentage ratings of shock occurrence for each stimulus. Finally, they made a forced choice of one stimulus paired with the shock. CS+, CS- and a fixation symbol were all presented as stimuli in the latter two questions. Observers completed this questionnaire after the direct-expression stage to avoid interfering with the learning process (Haaker, Golkar, et al., 2017).

Evaluation of the Demonstrator's Expression (the Observational US)

To control how the observers perceived the demonstrators' behavior, we used a set of questions suggested by Haaker, Golkar, et al. (2017). At the end of the experiment, we asked the observers to rate: how much discomfort the demonstrator experienced when receiving the

electrical stimulation, how expressive the demonstrator was, how natural the demonstrator's reactions were, and how much empathy they felt for the demonstrator. Additionally, we asked the observers to rate the degree of unpleasantness attributed to the demonstrators. Finally, in the 'friend' group, the observer scored the degree to which they identified with their friend. All ratings used a 10-point Likert scale, ranging from 0 (*not at all*) to 9 (*very much*), except for the unpleasantness rating, which used a 5-point Likert scale ranging from 1 (*very unpleasant*) to 5 (*very pleasant*).

Skin Conductance Response Recordings

During fMRI sessions, we registered skin conductance responses as a secondary measure. It was recorded using BrainVision BrainAmp ExG MR amplifier with GSR MR sensor, sampled at 250 Hz.

fMRI Data Acquisition

The MRI data were acquired on a 3T Siemens Magnetom Trio scanner equipped with a 12 channel head coil. At the beginning of a session, a T1-weighted anatomical image was acquired using an MPRAGE sequence with 1 × 1 × 1 mm resolution and the following parameters: inversion time TI = 1100 ms, GRAPPA parallel imaging with acceleration factor PE = 2, acquisition time TA = 6 minutes and 3 seconds. After acquiring the anatomical scans, two functional imaging runs followed (observational learning and direct-expression tasks). The first run contained 362 volumes in the ‘friend’ group and 380 volumes in the ‘stranger’ group. The scanning started earlier in the 'stranger' group, but the leading volumes were removed from the analysis. The second run of scanning contained 184 volumes. Each functional volume comprised 47 axial slices (2.3 mm thick, with 2.3 × 2.3 mm in-plane resolution and 30% distance factor) that were acquired using a T2*-sensitive gradient echo-planar imaging (EPI) sequence with the following parameters: repetition time TR = 2870 ms, echo time TE = 30 ms, flip angle FA = 90 degrees, field of view FoV = 212 mm, matrix size: 92 × 92, interleaved acquisition order, GRAPPA acceleration factor PA = 2.

fMRI Data Preprocessing

The fMRI data were preprocessed using fMRIPrep 1.4.0 (Esteban, Blair, et al., 2019; Esteban, Markiewicz, et al., 2019), based on Nipype 1.2.0 (Gorgolewski et al., 2011; Gorgolewski et al., 2019) and Nilearn 0.5.2 (Abraham et al., 2014). We followed the fMRIprep preprocessing with smoothing in SPM (SPM 12 v7487, Wellcome Centre for Human Neuroimaging, London, UK). At the beginning of the fMRIprep pipeline, the anatomical images were corrected for intensity non-uniformity with N4BiasFieldCorrection (Tustison et al., 2010), distributed with ANTs 2.2.0 (Avants et al., 2008), and used as an anatomical reference. The anatomical reference was then skull-stripped with antsBrainExtraction (from ANTs) and segmented using fast from FSL 5.0.9 (Zhang et al., 2001). Finally, the anatomical images were normalized to the MNI space through nonlinear registration with antsRegistration (ANTs 2.2.0). The ICBM 152 Nonlinear Asymmetrical template version 2009c was used (Fonov et al., 2009).

The functional images from the observational learning and direct-expression stages were preprocessed in the following manner. First, a reference volume was generated using a custom methodology of fMRIPrep. This reference was co-registered to the anatomical reference using flirt from FSL 5.0.9 (Jenkinson & Smith, 2001) with the boundary-based registration cost-function (Greve & Fischl, 2009). Head-motion parameters with respect to the functional reference volume (transformation matrices and six corresponding rotation and translation parameters) were estimated before any spatiotemporal filtering using mcflirt from FSL 5.0.9 (Jenkinson et al., 2002). The functional scanning runs were slice-time corrected using 3dTshift from AFNI 20160207 (Cox & Hyde, 1997). Next, the functional images were resampled into the MNI space. All resamplings were performed in a single interpolation step (composing head-motion transform matrices and co-registrations to anatomical and output spaces) using antsApplyTransforms (ANTs). Finally, we smoothed the functional images with a 6 mm FWHM 3D Gaussian kernel using spm_smooth (SPM 12). Framewise displacement (FD) and the derivative of root mean square variance over voxels (DVARS) were calculated by fMRIPrep for each functional scan, both using their implementations in Nipype and following

674 the definitions by (Power et al., 2014). Frames that exceeded a threshold of 0.5 mm FD or 1.5
675 standardized DVARS were annotated as motion outliers. For more details on the fMRIprep
676 pipeline, see fMRIPrep's documentation at https://fmriprep.org/en/latest/workflows.html.
677
678 **Physiological Data Analysis**
679 To analyze skin conductance data we used PsPM 4.3.0 software
680 (https://bachlab.github.io/PsPM/) running under MATLAB 2018b (MathWorks, Natick, MA,
681 USA). We used a non-linear model for event-related SCR. In this analysis, three parameters
682 of sudomotor nerve response function (its amplitude, latency and dispersion) are estimated to
683 best match the observed skin conductance data. This model is suitable for anticipatory
684 responses in fear conditioning and assumes that the response onset following CS presentation
685 is not precisely known (Bach et al., 2010; Staib et al., 2015). Before the analysis, we visually
686 inspected the signals for artifacts and manually marked missing epochs. We excluded subjects
687 with missing data or excessive presence of artifacts precluding further analysis. As a result,
688 we analyzed SCR data for 27 subjects per group. We used the default settings for
689 preprocessing: signals were filtered using bi-directional 1st order Butterworth filters, with 5 Hz
690 low-pass and 0.0159 Hz high-pass cut-off frequencies, and resampled to 10 Hz. We performed
691 no response normalization. We accelerated the processing of multiple subjects using GNU
692 Parallel v.20161222 (Tange, 2011).
693
694 **fMRI Data Analysis**
695 ***Activation Analysis***
696 To analyze data we used a mass univariate approach based on a general linear model.
697 We used SPM 12 software (SPM 12 v7487, Wellcome Centre for Human Neuroimaging,
698 London, UK) running under MATLAB 2020a (MathWorks, Natick, MA, USA). First-level models
699 contained four types of events in the observational learning stage: CS+, CS-, US, and no US
700 (i.e., lack of US during 50% of CS+). The observational CS were modeled as instantaneous
701 events (i.e., CS onset), while the observational US/no US events were 1.5 seconds (i.e., from

US onset to CS offset). There were only two types of events in the direct-expression stage, CS+ and CS-, modeled as 9 seconds (entire presentation of CS). Additionally, we included temporal modulation of the 1st order to capture effects of extinction in the direct-expression stage. In addition to the event regressors described above, we had six motion parameters (translation and rotation) as regressors of no interest. We added one delta regressor for each volume annotated by fMRIPrep as a motion outlier (up to 60 such volumes per subject in the observational learning stage, up to 38 in the direct-expression stage, median 8 and 2, respectively).

The US > no US was the primary contrast of interest in the observational learning stage and the CS+ > CS- in the direct-expression stage. We calculated the contrasts within-subject and used the parameter estimates in second-level analyses. We performed two types of second-level analyses in SPM: one-sample t-test designs for data pooled across groups (the 'friend' and 'stranger' groups) and two-sample t-tests for between-groups comparisons (the 'friend' vs. the 'stranger' group). Additionally, we used a temporal modulation regressor (CS+ × t) for both groups analyzed together and for between-group comparisons. We thresholded the second-level statistical maps using family-wise error (FWE) correction, with a $p = 0.05$ threshold. We used the voxel-level correction for the primary contrasts and cluster size correction with $p = .001$ cluster defining threshold for the results of temporal modulation and psychophysiological interactions.

Region-of-interest - Definitions and Analysis

To perform the ROI analysis (parameter estimate extraction), the psychophysiological interaction analysis (time course extraction), and, in the case of the amygdala, the small volume correction (SVC) analysis, we defined anatomical regions of interest (ROI). We used the following brain structures as ROIs: the anterior insula (AI), anterior mid-cingulate cortex (aMCC), amygdala, fusiform face area (FFA), right posterior superior temporal sulcus (rpSTS), and right temporo-parietal junction (rTPJ). We chose regional definitions for these structures based on a meta-analytic connectivity mapping study focusing on social processes

730 (Gorgolewski et al., 2011) and the Neurovault collection
731 (https://identifiers.org/neurovault.collection:2462).
732 We combined anatomical masks from the left and right hemispheres and treated them
733 as single ROIs in the AI, amygdala, and FFA analysis. For the TPJ and pSTS, the regions
734 considered functionally lateralized (Alcalá-López et al., 2018; Boccadoro et al., 2019; Sliwinska
735 & Pitcher, 2018), we used only the right-hemispheric masks. For the aMCC, which is a
736 centrally-located structure, we used no hemispheric division. We used the same definitions
737 across the ROI and PPI analyses. For small volume correction, which was applied only for the
738 amygdala, we used an alternative bilateral definition based on the Harvard - Oxford atlas
739 (Desikan et al., 2006) thresholded at 0.7. This definition was consistent with a previous study
740 on observational fear conditioning (Lindström et al., 2018) and provided better structure
741 coverage than the more restrictive meta-analytic definition. For the ROI analysis, the first-level
742 parameter estimates were extracted and averaged within a given region for each participant
743 using the spm_summarise function from SPM and compared using the BayesFactor package
744 in R (Morey & Rouder, 2018).
745
746 ***Psychophysiological Interactions***
747 To perform the psychophysiological interaction analysis (PPI), we extracted the
748 functional time series (1st eigenvariate) from the ROIs defined above and multiplied with the
749 psychological variable (observation stage: US > no US; direct-expression stage: CS+ > CS-)
750 using SPM VOI and PPI modules. We entered the PPI time series into a first-level model as
751 the regressor of interest. We also included the functional time series and the psychological
752 variable in the model as regressors and the motion parameters and motion outliers (the same
753 as in the models used for activation analysis). Then we subjected parameter estimates
754 obtained for the PPI regressor to second level analyses, using one-sample (both groups
755 analyzed together) and two-sample (between-group) designs. We thresholded the statistical
756 maps using cluster-based FWE correction, with cluster-defining threshold of $p = 0.001$ and
757 corrected p-value of 0.05. Additionally, we applied a small volume correction to the amygdala.

Statistical Analysis

To perform most statistical analyses we used R with *afex*, *emmeans*, and *BayesFactor* libraries, with plots made using *the ggpubr* library. We calculated Bayesian ANOVA using JASP. We used repeated-measures ANOVA (with type III errors) and Bayesian repeated-measures ANOVA to analyze STAI-state scores (with the group as a between-subject factor and the questionnaire filling time, before and after the experiment, as a within-subject factor) and skin conductance response amplitudes (with the group and stimulus factors). We used the Wilcoxon-Mann-Whitney test to compare the discrete ratings describing the demonstrator's expression (observational US) between the groups and a chi-squared test to compare the distribution of contingency-aware participants. We used t-test (with Welch's correction for unequal variance) and Bayesian t-test (using default effect size priors, i.e., Cauchy scale 0.707) to compare the results of STAI-trait and subscales of SWE, and region-of-interest parameter estimates from fMRI.

For the classical tests, we applied a significance level of $p = 0.05$. For Bayesian t-tests, we used BF10 to denote evidence for the alternative hypothesis and BF01 for the null hypothesis. In Bayesian ANOVA, we reported the effects as the Bayes factor for the inclusion of a given effect (BFincl), calculated as a ratio between the models' average likelihood, including the factor (given the data) vs. that of the models without the factor. When interpreting these results, we followed the convention suggested by Keysers et al. (2020) and considered $\frac{1}{3} < BF < 3$ as absence of evidence, $1/10 < BF < \frac{1}{3}$ or $3 < BF < 10$ as moderate evidence and $BF < 1/10$ or $BF > 10$ as strong evidence.

Data Availability

Relevant data are stored in an OSF repository and are available at https://osf.io/g3wkq/. Unthresholded statistical maps from the reported comparisons are also available at Neurovault, https://neurovault.org/collections/RSLLSFTQ/. Code replicating analyses reported here is available at https://github.com/nencki-lobi/emocon-mri.

Acknowledgements

We thank Jan Haaker for his valuable advice regarding the protocol's modifications. We also acknowledge Urszula Baranowska and Małgorzata Dąbkowska for their support in collecting data. Data collection and analysis were sponsored by National Science Centre grant 2015/19/B/HS6/02209. Ewelina Knapska was supported by European Research Council Starting Grant (H 415148).

Competing Interests

The authors declare no competing interests.

Author Contributions

Anna M. Kaźmierowska - Conceptualization, Methodology, Data curation, Formal Analysis, Investigation, Software, Visualization, Writing - original draft, Writing - review & editing

Michał Szczepanik - Conceptualization, Methodology, Data curation, Formal Analysis, Investigation, Software, Visualization, Writing - original draft, Writing - review & editing

Marek Wypych - Conceptualization, Methodology, Supervision, Writing - review & editing

Dawid Droździel - Investigation, Resources

Artur Marchewka - Conceptualization, Methodology, Resources, Supervision, Writing - review & editing

Jarosław M. Michałowski - Conceptualization, Methodology, Supervision, Writing - review & editing

Andreas Olsson - Conceptualization, Supervision, Writing - review & editing

Ewelina Knapska - Conceptualization, Methodology, Funding acquisition, Project administration, Supervision, Writing - review & editing

Appendix

Table S1

Evaluation of the Demonstrator's Expression (the Observational US)

	Discomfort of the Demonstrator		Expressiveness of the Demonstrator		Naturalness of the Demonstrator		Empathy Toward the Demonstrator		Identifying with the Demonstrator		Unpleasantness Attributed to the Demonstrator	
Group	F	S	F	S	F	S	F	S	F	S	F	S
Median (IQR)	6 (2.0)	6 (2.0)	6 (2.0)	6.5 (2.0)	7 (4.0)	7 (3.75)	5 (3.5)	5 (3.75)	7 (2.0)	n/a *	1 (1.0)	2 (1.0)
Range	2 - 8	0 - 9	2 - 8	4 - 9	0 - 9	2 - 9	0 - 9	0 - 8	1 - 9	n/a	1 - 4	1 - 5
Stat. Test	W = 581.5, p = 0.87		W = 501, p = 0.25		W = 630.5, p = 0.67		W = 671.5, p = 0.36		n/a		W = 586, p = 0.91	

Note. To evaluate the demonstrator's expression (the observational US), we asked the observers to rate (on a 0 - 9 scale) the demonstrator's reactions. The questions concerned the demonstrator's responses to electrical stimulation (how much discomfort they experienced, how expressive they were, and how natural their reactions were) and the observers' attitude (how much empathy they felt for the demonstrator). Additionally, we asked the observers how well they could identify with the demonstrator. We asked the question in the pairs of friends only, as the pilot studies revealed problems with the question's understanding in the 'stranger' group (*n/a: no answer). Additionally, we asked the observers to rate the degree of unpleasantness attributed to the demonstrators (on a 1 - 5 scale). The last row shows comparisons between the 'friend' and 'stranger' groups, the Wilcoxon-Mann-Whitney test, p-values uncorrected. F - 'friend' group; S - 'stranger' group; IQR: interquartile range.

Table S2

Descriptive Statistics for Age, Demonstrator-observer Friendship Length and the McGill Friendship Questionnaire (MFQ) Result for the Subgroups of Participants

Variable	Subgroup	Mean (SD)	Median (IQR)	Range
Age	OF	22.5 (2.77)	22 (4.5)	18 - 29

	OS	23.3 (2.95)	22.5 (4)	18 - 30
	D	22.1 (2.53)	22 (4)	18 - 28
Friendship Length	OF	7.7 (4.22)	6 (7)	3 - 19
MFQ Result	OF	52 (7.7)	55 (9.5)	33 - 60
	DF	49.8 (9.21)	52.5 (15)	30 - 60

Note. Data regarding friendship length and the MFQ result were collected in the 'friend' group only. OF: observers from the 'friend' group who learned the contingency (n = 35); OS: observers from the 'stranger' group who learned the contingency (n = 34); D: demonstrators for whom either a friend or a stranger observer learned the contingency (n = 44); DF: demonstrators for whom a friend observer learned the contingency (n = 34); SD: standard deviation; IQR: interquartile range.

Table S3

Activation Peaks in the Observational Learning Stage, US > no US Contrast

Cluster	Peak x	Peak y	Peak z	Peak value	Volume mm	Vox	Label
1	50	-66	6	14.98	89912	11239	Right Lateral Occipital Cortex inferior division
	44	-76	-8	12.92			Right Lateral Occipital Cortex inferior division
	42	-44	-16	12.21			Right Temporal Occipital Fusiform Cortex
	64	-40	26	11.94			Right Supramarginal Gyrus posterior division
	52	-28	-6	11.74			Right Middle Temporal Gyrus posterior division
	50	-40	10	11.51			Right Supramarginal Gyrus posterior division
	34	22	-18	10.71			Right Frontal Orbital Cortex
	52	8	-22	10.34			Right Temporal Pole
	22	-88	-8	10.07			Right Occipital Fusiform Gyrus
	46	26	-4	9.82			Right Frontal Orbital Cortex
	42	-2	-14	9.71			Right Planum Polare
	52	24	22	9.14			Right Inferior Frontal Gyrus pars opercularis

	46	2	44	8.88			Right Precentral Gyrus
	12	-68	38	8.81			Right Precuneous Cortex
	36	-62	-20	8.55			Right Occipital Fusiform Gyrus
	22	-2	-18	8.42			Right Amygdala
	14	-98	6	8.17			Right Occipital Pole
	28	-92	12	8.16			Right Occipital Pole
	38	6	4	7.50			Right Insular Cortex
	54	40	-2	7.40			Right Frontal Pole
	64	-32	40	7.35			Right Supramarginal Gyrus anterior division
	26	-80	34	6.78			Right Lateral Occipital Cortex superior division
2	-48	-78	6	13.87	32568	4071	Left Lateral Occipital Cortex inferior division
	-52	-58	10	11.73			Left Middle Temporal Gyrus temporooccipital part
	-62	-46	22	11.32			Left Supramarginal Gyrus posterior division
	-44	-50	-18	10.52			Left Inferior Temporal Gyrus temporooccipital part
	-30	-92	-10	9.49			Left Occipital Pole
	-24	-66	-28	6.64			no label
	-28	-94	14	6.22			Left Occipital Pole
3	-32	20	-14	10.65	15520	1940	Left Frontal Orbital Cortex
	-30	28	2	8.87			Left Insular Cortex
	-42	0	-16	8.24			Left Planum Polare
	-38	-12	-6	8.12			Left Insular Cortex
	-20	-4	-14	7.58			Left Amygdala
	-54	10	8	6.42			Left Inferior Frontal Gyrus pars opercularis
4	6	20	38	9.50	10368	1296	Right Paracingulate Gyrus
	4	20	56	9.07			Right Superior Frontal Gyrus
	6	40	10	8.55			Right Cingulate Gyrus anterior division
	10	4	72	6.61			Right Superior Frontal Gyrus
5	-8	-24	-12	9.77	6816	852	Brain-Stem
	12	-22	-10	8.72			no label

	10	-8	6	8.38			Right Thalamus
	10	8	4	7.85			Right Caudate
	6	-4	-10	7.13			no label
6	-10	-66	36	8.61	2336	292	Left Precuneous Cortex
7	-2	-24	28	8.69	2096	262	Left Cingulate Gyrus posterior division
	0	-8	32	6.43			Left Cingulate Gyrus anterior division
8	-16	-94	26	7.12	1896	237	Left Occipital Pole
	-26	-78	24	5.95			Left Lateral Occipital Cortex superior division
9	34	-52	50	6.78	1072	134	Right Superior Parietal Lobule
10	-30	-52	52	6.86	680	85	Left Superior Parietal Lobule
11	4	52	34	6.47	632	79	Right Superior Frontal Gyrus
12	-10	-76	-44	6.58	440	55	no label
13	-10	-84	8	6.03	392	49	Left Intracalcarine Cortex
14	-40	-4	48	6.68	376	47	Left Precentral Gyrus
15	-50	-26	-6	7.12	368	46	Left Middle Temporal Gyrus posterior division

Note. Table shows local maxima more than 16 mm apart. For brevity, clusters greater than 30 voxels were included. Last column gives the most probable label from the Harvard - Oxford atlas.

Table S4

Activation Peaks in the Direct-expression Stage, CS+ > CS- Contrast

Cluster	Peak x	Peak y	Peak z	Peak value	Volume mm	Vox	Label
1	30	30	0	8.30	5024	628	Right Frontal Orbital Cortex
	50	22	4	6.70			Right Inferior Frontal Gyrus pars triangularis
2	-36	24	-4	7.18	1400	175	Left Frontal Orbital Cortex
3	-14	-76	-30	6.37	112	14	no label
4	10	-12	-12	6.25	64	8	no label
5	6	24	36	5.77	40	5	Right Paracingulate Gyrus
6	34	46	20	5.63	8	1	Right Frontal Pole
7	8	4	2	5.45	8	1	Right Caudate

845 *Note.* Table shows local maxima more than 16 mm apart. Last column gives the most probable

846 label from the Harvard - Oxford atlas.

847

848 **Table S5**

849 *Activation Peaks for the Temporal Modulation of the CS+ Response in the Direct-Expression*

850 *Stage*

Cluster	Peak x	Peak y	Peak z	Peak value	Volume mm	Vox	Label
					Both Groups		
1	-18	-88	-6	6.38	10480	1310	Left Occipital Fusiform Gyrus
	-8	-100	0	5.43			Left Occipital Pole
	-12	-80	-32	4.49			no label
	10	-86	-10	4.47			Right Lingual Gyrus
	0	-86	4	4.01			Left Intracalcarine Cortex
	24	-76	-14	3.65			Right Occipital Fusiform Gyrus
	-26	-98	20	3.58			Left Occipital Pole
2	-4	-54	62	5.42	5344	668	Left Precuneous Cortex
	-12	-76	44	4.84			Left Lateral Occipital Cortex superior division
	4	-36	46	3.75			Right Cingulate Gyrus posterior division
	-8	-68	28	3.71			Left Precuneous Cortex
3	2	8	34	4.58	1704	213	Right Cingulate Gyrus anterior division
	-2	26	24	3.66			Left Cingulate Gyrus anterior division
4	44	28	8	4.71	1184	148	Right Inferior Frontal Gyrus pars triangularis
5	6	46	32	5.67	848	106	Right Paracingulate Gyrus
					Friend > Stranger		
1	-58	14	10	5.83	2280	285	Left Inferior Frontal Gyrus pars opercularis
2	-62	-44	8	4.65	1328	166	Left Supramarginal Gyrus posterior division
3	16	-58	-2	4.41	1096	137	Right Lingual Gyrus
4	-52	36	8	4.83	1072	134	Left Inferior Frontal Gyrus pars triangularis
5	-24	-6	12	4.55	768	96	Left Putamen

Note. Table shows local maxima more than 16 mm apart. Last column gives the most probable label from the Harvard - Oxford atlas.

Table S6

Activation peaks for the psychophysiological interaction analysis based on the US > no US contrast

Cluster	Peak x	Peak y	Peak z	Peak value	Volume mm	Vox	Label
					Anterior Insula		
1	64	-38	20	6.16	8520	1065	Right Supramarginal Gyrus posterior division
	54	-48	4	5.00			Right Middle Temporal Gyrus temporooccipital part
	58	-66	6	4.63			Right Lateral Occipital Cortex inferior division
	48	-28	2	4.62			Right Superior Temporal Gyrus posterior division
	48	-80	0	3.60			Right Lateral Occipital Cortex inferior division
2	-52	-56	12	5.26	6792	849	Left Middle Temporal Gyrus temporooccipital part
	-42	-70	12	4.80			Left Lateral Occipital Cortex inferior division
	-68	-46	8	4.01			Left Middle Temporal Gyrus temporooccipital part
	-50	-80	-4	3.76			Left Lateral Occipital Cortex inferior division
3	-12	-74	-14	4.88	3536	442	Left Lingual Gyrus
	-30	-74	-22	4.64			Left Occipital Fusiform Gyrus
	-40	-64	-14	3.66			Left Occipital Fusiform Gyrus
4	52	14	26	4.46	808	101	Right Inferior Frontal Gyrus pars opercularis
5	32	-68	-28	4.16	744	93	no label
					posterior STS		
1	46	-64	2	9.29	20656	2582	Right Lateral Occipital Cortex inferior division
	66	-40	20	6.51			Right Supramarginal Gyrus posterior division
	38	-80	-14	5.01			Right Lateral Occipital Cortex inferior division
	46	-40	10	4.64			Right Supramarginal Gyrus posterior division
	62	-38	44	4.21			Right Supramarginal Gyrus posterior division
	32	-94	-4	3.51			Right Occipital Pole
2	-46	-70	8	8.07	12424	1553	Left Lateral Occipital Cortex inferior division

	-58	-48	12	5.20			Left Supramarginal Gyrus posterior division
3	38	32	-2	5.68	4840	605	Right Frontal Orbital Cortex
4	-58	-40	36	4.70	3072	384	Left Supramarginal Gyrus posterior division
	-66	-32	24	4.63			Left Supramarginal Gyrus anterior division
5	-38	22	-8	5.01	2608	326	Left Frontal Orbital Cortex
	-34	6	-6	3.57			Left Insular Cortex
6	48	14	30	4.91	2240	280	Right Inferior Frontal Gyrus pars opercularis
	54	30	20	3.71			Right Inferior Frontal Gyrus pars triangularis
7	48	-42	-16	6.12	1992	249	Right Inferior Temporal Gyrus temporooccipital part
8	38	-12	-6	4.76	1768	221	Right Insular Cortex
	50	-24	-4	4.49			Right Middle Temporal Gyrus posterior division
9	12	-2	12	4.93	1664	208	Right Thalamus
	-2	-4	4	3.94			Left Thalamus
10	54	20	8	4.96	1520	190	Right Inferior Frontal Gyrus pars opercularis
11	6	6	62	4.63	1344	168	Right Juxtapositional Lobule Cortex (formerly Supplementary Motor Cortex)
12	20	10	-6	4.96	1120	140	Right Putamen
13	-4	-14	-10	4.75	904	113	no label
14	6	-24	0	4.49	816	102	Right Thalamus
15	-40	-62	-28	4.65	744	93	no label
posterior STS (small volume corrected within the amygdala)							
1	24	-4	-16	3.82	104	13	Right Amygdala
2	-22	-4	-14	3.56	24	3	Left Amygdala
3	-20	-6	-18	3.42	8	1	Left Amygdala

Note. Table shows local maxima more than 16 mm apart. Last column gives the most probable label from the Harvard - Oxford atlas.

References

Abraham, A., Pedregosa, F., Eickenberg, M., Gervais, P., Mueller, A., Kossaifi, J., Gramfort, A., Thirion, B., & Varoquaux, G. (2014). Machine learning for neuroimaging with scikit-learn. *Frontiers in Neuroinformatics*, *8*. https://doi.org/10.3389/fninf.2014.00014

Alcalá-López, D., Smallwood, J., Jefferies, E., Van Overwalle, F., Vogeley, K., Mars, R. B., Turetsky, B. I., Laird, A. R., Fox, P. T., Eickhoff, S. B., & Bzdok, D. (2018). Computing the Social Brain Connectome Across Systems and States. *Cerebral Cortex*, *28*(7), 2207–2232. https://doi.org/10.1093/cercor/bhx121

Allison, T., Puce, A., & McCarthy, G. (2000). Social perception from visual cues: role of the STS region. *Trends in Cognitive Sciences*, *4*(7), 267–278. https://doi.org/10.1016/s1364-6613(00)01501-1

Avants, B. B., Epstein, C. L., Grossman, M., & Gee, J. C. (2008). Symmetric diffeomorphic image registration with cross-correlation: Evaluating automated labeling of elderly and neurodegenerative brain. *Medical Image Analysis*, *12*(1), 26–41. https://doi.org/10.1016/j.media.2007.06.004

Bach, D. R., Daunizeau, J., Friston, K. J., & Dolan, R. J. (2010). Dynamic causal modelling of anticipatory skin conductance responses. *Biological Psychology*, *85*(1), 163–170. https://doi.org/10.1016/j.biopsycho.2010.06.007

Beckes, L., Coan, J. A., & Hasselmo, K. (2013). Familiarity promotes the blurring of self and other in the neural representation of threat. *Social Cognitive and Affective Neuroscience*, *8*(6), 670–677. https://doi.org/10.1093/scan/nss046

Boccadoro, S., Cracco, E., Hudson, A. R., Bardi, L., Nijhof, A. D., Wiersema, J. R., Brass, M., & Mueller, S. C. (2019). Defining the neural correlates of spontaneous theory of mind (ToM): An fMRI multi-study investigation. *NeuroImage*, *203*, 116193. https://doi.org/10.1016/j.neuroimage.2019.116193

Bruder, M., Dosmukhambetova, D., Nerb, J., & Manstead, A. S. R. (2012). Emotional signals in nonverbal interaction: dyadic facilitation and convergence in expressions, appraisals, and feelings. *Cognition & Emotion*, *26*(3), 480–502. https://doi.org/10.1080/02699931.2011.645280

Cheng, Y., Chen, C., Lin, C.-P., Chou, K.-H., & Decety, J. (2010). Love hurts: an fMRI study. *NeuroImage*, *51*(2), 923–929. https://doi.org/10.1016/j.neuroimage.2010.02.047

Cox, R. W., & Hyde, J. S. (1997). Software tools for analysis and visualization of fMRI data.

NMR in Biomedicine, *10*(4-5), 171–178. https://doi.org/10.1002/(SICI)1099-1492(199706/08)10:4/5<171::AID-NBM453>3.0.CO;2-L

Davis, M. H. (1983). Measuring individual differences in empathy: Evidence for a multidimensional approach. *Journal of Personality and Social Psychology*, *44*(1), 113–126. https://doi.org/10.1037/0022-3514.44.1.113

Desikan, R. S., Ségonne, F., Fischl, B., Quinn, B. T., Dickerson, B. C., Blacker, D., Buckner, R. L., Dale, A. M., Maguire, R. P., Hyman, B. T., Albert, M. S., & Killiany, R. J. (2006). An automated labeling system for subdividing the human cerebral cortex on MRI scans into gyral based regions of interest. *NeuroImage*, *31*(3), 968–980. https://doi.org/10.1016/j.neuroimage.2006.01.021

de Vignemont, F., & Singer, T. (2006). The empathic brain: how, when and why? *Trends in Cognitive Sciences*, *10*(10), 435–441. https://doi.org/10.1016/j.tics.2006.08.008

De Waal, F. B. M. (2012). The antiquity of empathy. *Science*, *336*(6083), 874–876. https://doi.org/10.1126/science.1220999

de Waal, F. B. M., & Preston, S. D. (2017). Mammalian empathy: behavioural manifestations and neural basis. *Nature Reviews. Neuroscience*, *18*(8), 498–509. https://doi.org/10.1038/nrn.2017.72

Esteban, O., Blair, R., Markiewicz, C. J., Berleant, S. L., Moodie, C., Ma, F., Isik, A. I., Erramuzpe, A., Kent, J. D., Goncalves, M., DuPre, E., Sitek, K. R., Gomez, D. E. P., Lurie, D. J., Ye, Z., Salo, T., Valabregue, R., Amlien, I. K., Liem, F., … Gorgolewski, K. J. (2019). *fMRIPrep: a robust preprocessing pipeline for functional MRI* (Version 1.4.0) [Computer software]. https://doi.org/10.5281/zenodo.2851559

Esteban, O., Markiewicz, C. J., Blair, R. W., Moodie, C. A., Isik, A. I., Erramuzpe, A., Kent, J. D., Goncalves, M., DuPre, E., Snyder, M., Oya, H., Ghosh, S. S., Wright, J., Durnez, J., Poldrack, R. A., & Gorgolewski, K. J. (2019). fMRIPrep: a robust preprocessing pipeline for functional MRI. *Nature Methods*, *16*(1), 111–116. https://doi.org/10.1038/s41592-018-0235-4

Fonov, V. S., Evans, A. C., McKinstry, R. C., Almli, C. R., & Collins, D. L. (2009). Unbiased

nonlinear average age-appropriate brain templates from birth to adulthood. *NeuroImage*, *47, Supplement 1*, S102. https://doi.org/10.1016/S1053-8119(09)70884-5

Fullana, M. A., Harrison, B. J., Soriano-Mas, C., Vervliet, B., Cardoner, N., Àvila-Parcet, A., & Radua, J. (2016). Neural signatures of human fear conditioning: an updated and extended meta-analysis of fMRI studies. *Molecular Psychiatry*, *21*(4), 500–508. https://doi.org/10.1038/mp.2015.88

Golkar, A., Castro, V., & Olsson, A. (2015). Social learning of fear and safety is determined by the demonstrator's racial group. *Biology Letters*, *11*(1), 20140817. https://doi.org/10.1098/rsbl.2014.0817

Golkar, A., & Olsson, A. (2017). The interplay of social group biases in social threat learning. *Scientific Reports*, *7*(1), 7685. https://doi.org/10.1038/s41598-017-07522-z

Gonzalez-Liencres, C., Juckel, G., Tas, C., Friebe, A., & Brüne, M. (2014). Emotional contagion in mice: the role of familiarity. *Behavioural Brain Research*, *263*, 16–21. https://doi.org/10.1016/j.bbr.2014.01.020

Gorgolewski, K., Burns, C. D., Madison, C., Clark, D., Halchenko, Y. O., Waskom, M. L., & Ghosh, S. S. (2011). Nipype: a flexible, lightweight and extensible neuroimaging data processing framework in python. *Frontiers in Neuroinformatics*, *5*, 13. https://doi.org/10.3389/fninf.2011.00013

Gorgolewski, K. J., Esteban, O., Markiewicz, C. J., Ziegler, E., Ellis, D. G., Jarecka, D., Notter, M. P., Johnson, H., Burns, C., Manhães-Savio, A., Hamalainen, C., Yvernault, B., Salo, T., Goncalves, M., Jordan, K., Waskom, M., Wong, J., Modat, M., Loney, F., … Ghosh, S. (2019). *nipy/nipype: 1.2.0*. https://doi.org/10.5281/zenodo.2685428

Greve, D. N., & Fischl, B. (2009). Accurate and robust brain image alignment using boundary-based registration. *NeuroImage*, *48*(1), 63–72. https://doi.org/10.1016/j.neuroimage.2009.06.060

Haaker, J., Golkar, A., Selbing, I., & Olsson, A. (2017). Assessment of social transmission of threats in humans using observational fear conditioning. *Nature Protocols*, *12*(7), 1378–1386. https://doi.org/10.1038/nprot.2017.027

Haaker, J., Yi, J., Petrovic, P., & Olsson, A. (2017). Endogenous opioids regulate social threat learning in humans. *Nature Communications*, *8*, 15495. https://doi.org/10.1038/ncomms15495

Hatfield, E., Bensman, L., Thornton, P. D., & Rapson, R. L. (2014). New perspectives on emotional contagion: A review of classic and recent research on facial mimicry and contagion. *Interpersona: An International Journal of Personal Relationships*, *8*(2), 159–179. https://doi.org/10.5964/ijpr.v8i2.162

Hernandez-Lallement, J., Gómez-Sotres, P., & Carrillo, M. (2020). Towards a unified theory of emotional contagion in rodents—A meta-analysis. *Neuroscience and Biobehavioral Reviews*. https://doi.org/10.1016/j.neubiorev.2020.09.010

Jenkinson, M., Bannister, P., Brady, M., & Smith, S. (2002). Improved Optimization for the Robust and Accurate Linear Registration and Motion Correction of Brain Images. *NeuroImage*, *17*(2), 825–841. https://doi.org/10.1006/nimg.2002.1132

Jenkinson, M., & Smith, S. (2001). A global optimisation method for robust affine registration of brain images. *Medical Image Analysis*, *5*(2), 143–156. https://doi.org/10.1016/S1361-8415(01)00036-6

Jeon, D., Kim, S., Chetana, M., Jo, D., Ruley, H. E., Lin, S.-Y., Rabah, D., Kinet, J.-P., & Shin, H.-S. (2010). Observational fear learning involves affective pain system and Cav1.2 Ca2+ channels in ACC. *Nature Neuroscience*, *13*(4), 482–488. https://doi.org/10.1038/nn.2504

Kaźmierczak, M., Plopa, M., & Retowski, S. (2007). Skala wrażliwości empatycznej. *Przegląd Psychologiczny*, *50*(1), 9–24. https://www.kul.pl/files/714/nowy_folder/1.50.2007_art.1.pdf

Keysers, C., Gazzola, V., & Wagenmakers, E.-J. (2020). Using Bayes factor hypothesis testing in neuroscience to establish evidence of absence. *Nature Neuroscience*, *23*(7), 788–799. https://doi.org/10.1038/s41593-020-0660-4

Kiyokawa, Y., Honda, A., Takeuchi, Y., & Mori, Y. (2014). A familiar conspecific is more effective than an unfamiliar conspecific for social buffering of conditioned fear responses

in male rats. *Behavioural Brain Research*, *267*, 189–193. https://doi.org/10.1016/j.bbr.2014.03.043

Knapska, E., Mikosz, M., Werka, T., & Maren, S. (2010). Social modulation of learning in rats. *Learning & Memory* , *17*(1), 35–42. https://doi.org/10.1101/lm.1670910

Lindström, B., Haaker, J., & Olsson, A. (2018). A common neural network differentially mediates direct and social fear learning. *NeuroImage*, *167*, 121–129. https://doi.org/10.1016/j.neuroimage.2017.11.039

Mendelson, M. J., & Aboud, F. E. (1999). Measuring friendship quality in late adolescents and young adults: McGill Friendship Questionnaires. *Canadian Journal of Behavioural Science/Revue Canadienne Des Sciences Du Comportement*, *31*(2), 130. https://psycnet.apa.org/record/1999-13541-007

Morey, R. D., & Rouder, J. N. (2018). *BayesFactor: Computation of Bayes Factors for Common Designs* (Version 0.9.12-4.2). https://CRAN.R-project.org/package=BayesFactor

Olsson, A., Knapska, E., & Lindström, B. (2020). The neural and computational systems of social learning. *Nature Reviews. Neuroscience*, *21*(4), 197–212. https://doi.org/10.1038/s41583-020-0276-4

Olsson, A., Nearing, K. I., & Phelps, E. A. (2007). Learning fears by observing others: the neural systems of social fear transmission. *Social Cognitive and Affective Neuroscience*, *2*(1), 3–11. https://doi.org/10.1093/scan/nsm005

Olsson, A., & Phelps, E. A. (2007). Social learning of fear. *Nature Neuroscience*, *10*(9), 1095–1102. https://doi.org/10.1038/nn1968

Phelps, E. A., & LeDoux, J. E. (2005). Contributions of the amygdala to emotion processing: from animal models to human behavior. *Neuron*, *48*(2), 175–187. https://doi.org/10.1016/j.neuron.2005.09.025

Power, J. D., Mitra, A., Laumann, T. O., Snyder, A. Z., Schlaggar, B. L., & Petersen, S. E. (2014). Methods to detect, characterize, and remove motion artifact in resting state fMRI. *NeuroImage*, *84*(Supplement C), 320–341.

https://doi.org/10.1016/j.neuroimage.2013.08.048

Preston, S. D., & de Waal, F. B. M. (2002). Empathy: Its ultimate and proximate bases. *The Behavioral and Brain Sciences*, *25*(1), 1–20; discussion 20–71. https://doi.org/10.1017/s0140525x02000018

Proverbio, A. M. (2021). Sex differences in the social brain and in social cognition. *Journal of Neuroscience Research*. https://doi.org/10.1002/jnr.24787

Sanders, J., Mayford, M., & Jeste, D. (2013). Empathic fear responses in mice are triggered by recognition of a shared experience. *PloS One*, *8*(9), e74609. https://doi.org/10.1371/journal.pone.0074609

Sevenster, D., Beckers, T., & Kindt, M. (2014). Fear conditioning of SCR but not the startle reflex requires conscious discrimination of threat and safety. *Frontiers in Behavioral Neuroscience*, *8*, 32. https://doi.org/10.3389/fnbeh.2014.00032

Sliwinska, M. W., & Pitcher, D. (2018). TMS demonstrates that both right and left superior temporal sulci are important for facial expression recognition. *NeuroImage*, *183*, 394–400. https://doi.org/10.1016/j.neuroimage.2018.08.025

Spielberger, C. D., Gorsuch, R. L., Lushene, R., Vagg, P. R., & Jacobs, G. A. (1983). *Manual for the State-Trait Anxiety Inventory*. Consulting Psychologists Press.

Spielberger, C. D., Strelau, J., Tysarczyk, M., & Wrześniewski, K. (2012). *STAI - Inwentarz Stanu i Cechy Lęku*. Pracownia Testów Psychologicznych Polskiego Towarzystwa Psychologicznego.

Staib, M., Castegnetti, G., & Bach, D. R. (2015). Optimising a model-based approach to inferring fear learning from skin conductance responses. *Journal of Neuroscience Methods*, *255*, 131–138. https://doi.org/10.1016/j.jneumeth.2015.08.009

Szczepanik, M., Kaźmierowska, A. M., Michałowski, J. M., Wypych, M., Olsson, A., & Knapska, E. (2020). Observational learning of fear in real time procedure. *Scientific Reports*, *10*(1), 16960. https://doi.org/10.1038/s41598-020-74113-w

Tange, O. (2011). GNU Parallel - The Command-Line Power Tool. *;login: The USENIX Magazine*, *36*(1), 42–47. http://www.gnu.org/s/parallel

Tustison, N. J., Avants, B. B., Cook, P. A., Zheng, Y., Egan, A., Yushkevich, P. A., & Gee, J. C. (2010). N4ITK: Improved N3 Bias Correction. *IEEE Transactions on Medical Imaging*, *29*(6), 1310–1320. https://doi.org/10.1109/TMI.2010.2046908

Weidemann, G., Satkunarajah, M., & Lovibond, P. F. (2016). I Think, Therefore Eyeblink: The Importance of Contingency Awareness in Conditioning. *Psychological Science*, *27*(4), 467–475. https://doi.org/10.1177/0956797615625973

Yang, D. Y.-J., Rosenblau, G., Keifer, C., & Pelphrey, K. A. (2015). An integrative neural model of social perception, action observation, and theory of mind. *Neuroscience and Biobehavioral Reviews*, *51*, 263–275. https://doi.org/10.1016/j.neubiorev.2015.01.020

Zhang, Y., Brady, M., & Smith, S. (2001). Segmentation of brain MR images through a hidden Markov random field model and the expectation-maximization algorithm. *IEEE Transactions on Medical Imaging*, *20*(1), 45–57. https://doi.org/10.1109/42.906424